The Glyoxylate Cycle in Arbuscular Mycorrhizal Fungi. Carbon Flux and Gene Expression

Peter J. Lammers, Jeongwon Jun, Jehad Abubaker, Raul Arreola, Anjali Gopalan, Berta Bago[1], Cinta Hernandez-Sebastia[2], James W. Allen, David D. Douds, Philip E. Pfeffer, and Yair Shachar-Hill*

Department of Chemistry and Biochemistry, New Mexico State University, Las Cruces, New Mexico 88001 (P.J.L., J.J., J.A., R.A., A.G., C.H.-S., J.W.A., Y.S.-H.); and United States Department of Agriculture, Agricultural Research Service Eastern Regional Research Center, 600 East Mermaid Lane, Wyndmoor, Pennsylvania 19038 (B.B., D.D.D., P.E.P.)

AQ: A

The arbuscular mycorrhizal (AM) symbiosis is responsible for huge fluxes of photosynthetically fixed carbon from plants to the soil. Lipid, which is the dominant form of stored carbon in the fungal partner and which fuels spore germination, is made by the fungus within the root and is exported to the extraradical mycelium. We tested the hypothesis that the glyoxylate cycle is central to the flow of carbon in the AM symbiosis. The results of ^{13}C labeling of germinating spores and extraradical mycelium with $^{13}C_2$-acetate and $^{13}C_2$-glycerol and analysis by nuclear magnetic resonance spectroscopy indicate that there are very substantial fluxes through the glyoxylate cycle in the fungal partner. Full-length sequences obtained by polymerase chain reaction from a cDNA library from germinating spores of the AM fungus *Glomus intraradices* showed strong homology to gene sequences for isocitrate lyase and malate synthase from plants and other fungal species. Quantitative real-time polymerase chain reaction measurements show that these genes are expressed at significant levels during the symbiosis. Glyoxysome-like bodies were observed by electron microscopy in fungal structures where the glyoxylate cycle is expected to be active, which is consistent with the presence in both enzyme sequences of motifs associated with glyoxysomal targeting. We also identified among several hundred expressed sequence tags several enzymes of primary metabolism whose expression during spore germination is consistent with previous labeling studies and with fluxes into and out of the glyoxylate cycle.

Fn1

The arbuscular mycorrhizal (AM) symbiosis is ancient (Simon et al., 1993; Taylor et al., 1995; Redecker et al., 2000), widespread (Smith and Read, 1997), and vital to the life of plants. The majority of land plants rely on AM fungi to facilitate the uptake of phosphorus and other mineral nutrients from the soil. In return, the fungal partner receives photosynthetically fixed carbon. Comparisons of mycorrhizal with nonmycorrhizal plants of a wide variety of plant and fungal species have demonstrated a substantially increased carbon flow to mycorrhizal versus nonmycorrhizal roots (for review, see Douds et al., 2000; Graham, 2000). This involves the flow of huge quantities of carbon globally so that the mechanisms of carbon movement in the symbiosis are of ecological and agricultural significance.

AQ: B

Analytical studies have identified forms of carbon stored by the fungus as lipids (Beilby and Kidby, 1980; Jabaji-Hare, 1988; Gaspar et al., 1997), trehalose (Bécard et al., 1991), and glycogen (Bonfante et al., 1994; Shachar-Hill et al., 1995). Enzymological studies have provided evidence for the activity of a number of fungal enzymes, including lipase (Gaspar et al., 1997), phosphatases (Ezawa et al., 1995; Kojima et al., 1998), succinate and malate dehydrogenase (MacDonald and Lewis, 1978; Saito, 1995), trehalase (Schubert and Wyss, 1995), peroxidase and catalase (Nemec, 1981), and Glc-6-P dehydrogenase (Saito, 1995). At the molecular genetic level, fungal genes for glyceraldehyde-3-P dehydrogenase (Franken et al., 1997), chitin synthase (Lanfranco et al., 1999), and phosphoglycerate kinase (Harrier et al., 1998) were recently identified. Such studies implicate glycolysis, tricarboxylic acid (TCA), the pentose phosphate pathway (PPP), and lipid synthesis and breakdown as being active and developmentally regulated in the fungus.

Studies using stable isotope labeling and nuclear magnetic resonance (NMR) spectroscopy (Shachar-Hill et al., 1995; Bago et al., 1999; Pfeffer et al., 1999) have extended our understanding of carbon transfer and metabolism in the fungus and lead to working models of carbon flows in the AM symbiosis (Bago et al., 2000). The relative extent of labeling observed in different carbon positions of lipids, carbohydrates, and amino acids after supplying metabolic precursors labeled in particular positions can be interpreted in terms of likely metabolic pathways active in the fungus. Together with the analytical and enzymo-

[1] Present address: Departamento de Microbiología del Suelo y Sistemas Simbióticos, Estación Experimental del Zaidín, calle Profesor Albareda, 1, 18008-Granada, Spain.

[2] Present address: Department of Crop Science and Botany, North Carolina State University, Raleigh, NC 27695–7631.

* Corresponding author; e-mail yairhill@nmsu.edu; fax 505–646–3218.

Article, publication date, and citation information can be found at www.plantphysiol.org/cgi/doi/10.1104/pp.010375.

logical studies, the results of labeling experiments highlight the importance of lipids as the main storage form and an important export currency in the AM symbiosis. Triacylglyceride in particular is made in the intraradical parts of the fungus and is exported to the extraradical mycelium (Pfeffer et al., 1999). Supplying ^{13}C-labeled acetate to germinating spores or to the extraradical mycelium during symbiosis resulted in substantial labeling in fungal trehalose (Bago et al., 1999; Pfeffer et al., 1999), showing that gluconeogenesis is active in both these tissues. This result also suggests that the glyoxylate cycle may be central to the flow of carbon in the AM symbiosis (Bago et al., 2000). However, the interpretation of the labeling patterns is complicated by the sequential action of several pathways.

To confirm the activity of the glyoxylate cycle requires a demonstration that the genes for the two key enzymes of this pathway, isocitrate lyase (ICL; EC 4.1.3.1) and malate synthase (MS, EC 4.1.3.2), are expressed. Further labeling experiments are also required to confirm that carbon flows through the pathway. The regulation of metabolic gene expression in the AM symbiosis has yet to be analyzed (Harrison, 1999), and only a few genes of primary metabolism have even been identified in AM fungi (Franken et al., 1997; Harrier et al., 1998; Kaldorf et al., 1998). Therefore, we sought to identify ICL and MS genes and find out whether they are expressed, and we sought to provide functional evidence for flux through the glyoxylate cycle with ^{13}C-labeling experiments. The identification of ICL, MS, and other AM fungal metabolic genes reported here should allow the testing and extension of the recently proposed models of primary metabolism in the AM symbiosis (Bago et al., 2000, 2001).

RESULTS

Figure 1 shows ^{13}C NMR spectra of extracts of *G. intraradices* tissues that were incubated with $^{13}C_2$ glycerol (Fig. 1, A and B) or $^{13}C_2$ acetate (Fig. 1, C and D) while growing asymbiotically (Fig. 1, A and C, germinating spores) or symbiotically (Fig. 1, B and D, extraradical mycelium). As previously observed, the major metabolite signals in such spectra are those of ^{13}C-labeled trehalose (Bago et al., 1999; Pfeffer et al., 1999) because this is the major low-M_r carbohydrate in AM fungi (Bécard et al., 1991; Shachar-Hill et al., 1995). When $^{13}C_2$ glycerol is provided, trehalose becomes labeled mostly in C_2 and C_5: C_2 was labeled 25.0% in germinating spores and 14.4% in extracts of extraradical mycelium, whereas C_5 was labeled 37.5% and 27.1% in germinating spores and ex-

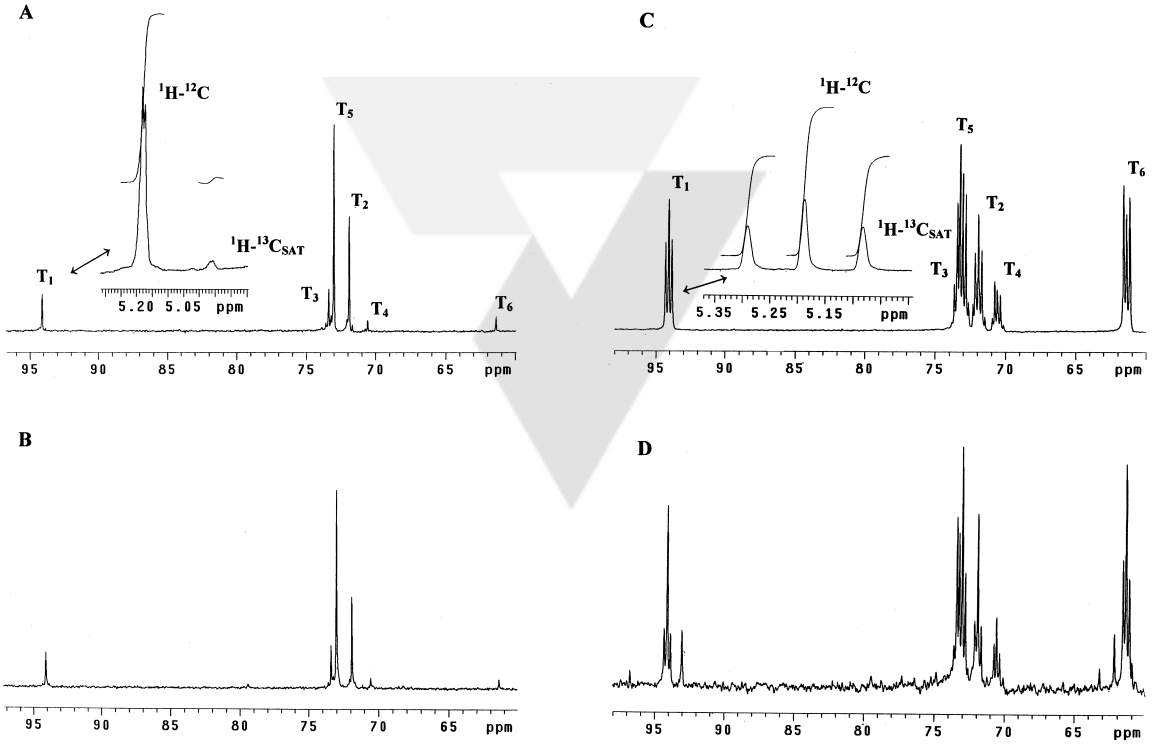

Figure 1. ^{13}C NMR spectra of extracts of germinating spores (A and C) and extraradical mycelium (B and D) of *Glomus intraradices* after incubation with ^{13}C-labeled substrates. $^{13}C_2$ glycerol (A and B) or $^{13}C_2$ acetate (C and D) was used. The signals from the six different positions of trehalose are labeled T1 through T6. Splitting of signals in C and D are due to the spectroscopic coupling in multiply labeled molecules. Insets in A and C are subsections of the ^{1}H spectra of the same samples. These insets show the ^{1}H signals from the anomeric (C1 and C1′) hydrogens of trehalose, including the ^{1}H-^{13}C satellite peaks whose areas relative to the central ^{1}H-^{12}C signals give the absolute percentage of ^{13}C levels in trehalose.

traradical mycelium, respectively (see "Materials and Methods" for an explanation of quantification of percentage of enrichments and replication). Labeling was also observed in glycogen and chitin from such tissues (not shown). These observations are consistent with active gluconeogenesis. We also observed labeling in C_1 and C_3 in trehalose from germinating spores (7.5% and 11.7%, respectively) and extraradical mycelium (5.0% and 7.3%, respectively) and much less in C_4 (2.4% and 2.0% in extraradical mycelium and germinating spores, respectively) or C_6 (1.2% and 0.5% in extraradical mycelium and germinating spores, respectively).

To test whether the primary source of carbon for gluconeogenesis is lipid, extraradical mycelium and germinating spores were exposed to $^{13}C_2$-acetate. High levels of labeling were observed in trehalose (Fig. 1, C and D), with carbons 1, 2, 5, and 6 of trehalose labeled to 55.6%, 55.8%, 73.9%, and 75.7%, respectively, in germinating spores, and 41.5%, 41.5%, 68.5%, and 75.0%, respectively, in the extraradical mycelium. High levels of multiple labeling led to multiple peaks for each carbon position. The lowest levels of labeling after exposure to $^{13}C_2$ acetate were seen in C_4 of trehalose (Fig. 1, C and D, 18.6% and 18.7% in germinating spores and extraradical mycelium, respectively). The C_3 position was labeled to 37.4% in germinating spores and 26.3% in extraradical mycelium. These labeling patterns are consistent with fluxes through the glyoxylate cycle (see below for discussion of labeling patterns).

Operation of the glyoxylate cycle requires the action of two key enzymes: ICL and MS. The sequences of these enzymes in *G. intraradices* were determined following PCR-based cloning of fragments from cDNA from germinating spores and further PCR-based cloning to obtain full-length sequence information (see "Materials and Methods"). Figures 2 and 3 F3 show multiple alignments of the ICL and MS amino acid sequences from *G. intraradices*. The *G. intraradices*

```
C. cinereus     ------------MSSERAQFASEVAEVERWWKSPRFARVNRPYTAADVVSKRG-TIKINYPSDVQGKKLWKLLSEHAKNGTPSHTYGALDPVQVTKMAKYLETVYVSGWQS
E. gossypii     -MSPSVRDARNDLASLQQQAAAEAEDIRRWWSQPRWAGTKRVYTAEDIVKRRGTFPVVEYPSSVMADKLVETLARHSRNGTVSQTFGVLDPVQMTQMVKYLDTIYVSGWQC
E. nidulans     ----------MSYIEEEDQRYWDEVAVKNWWKDSRWRYTKRPFTAEQIVAKRG-NLKIEYPSNVQAKKLWGILERNFKNKEASFTYGCLDPTMVTQMAKYLDTVYVSGWQS
N. crassa       MAANNMVNPAVDPALEDELFAKEVEEVKKWWSDSRWRQTKRPFTAEQIVSKRG-NLKIEYASNAQAKKLWKILEDRFAKRDASYTYGCLEPTMVTQMAKYLDTVYVSGWQS
S. cerevisiae   -MPIPVGNTKNDFAALQAKLDADAAEIEKWWSDSRWSKTKRNYSARDIAVRRGTFPPIEYPSSVMARKLFKVLEKHHNEGTVSKTFGALDPVQISQMAKYLDTIYISGWQC
G. intraradices ------MSSRDFIAQEQAAFEYEVAEVERWWQSDRFRLVKRPYTAEQIVSKRG-LLKQQYASDAQAKKLWSLFKRHQKNKTATHTFGALDPIQVAQMAKYLETVYVSGWQC
                              :  :..**.. *:  .:* ::* ::. :**     :*.*.. . **  :  .  :    : *:* *:*  :::*.***:*:*:****.


C. cinereus     SSTASSSNEPGPDLADYPSNTVPNKVEHLFMAQLFHDRKQREARSRMS--DAELANTPVIDYLRPIVADADTGHGGLTAVMKLTKMFVEKGAAGIHIEDQAPGTKKCGHMA
E. gossypii     SATASTSNEPGPDLADYPMDTVPNKVEHLFMAQLFHDRKQREARLSCTTQRELDQLGPEIDYLRPIVADADTGHGGLTAVFKLTKMFIERGAAGIHMEDQSSSNKKCGHMA
E. nidulans     SSTASSTDEPSPDLADYPMNTVPNKVNHLWMAQLFHDRKQREERMTTP--KDQRHKVTNVDYLRPIIADADTGHGGLTAVMKLTKLFVERGAAGIHIEDQAPGTKKCGHMA
N. crassa       SSTASSSDEPGPDLADYPYTTCPNKVGHLFMAQLFHDRKQRQERLSVP--KDQREKLANIDYLRPIVADADTGHGGLTAVMKLTKLFIEKGAAGIHIEDQAPGTKKCGHMA
S. cerevisiae   SSTASTSNEPGPDLADYPMDTVPNKVEHLFKAQLFHDRKQLEARSKAKSQEELDEMGAPIDYLTPIVADADAGHGGLTAVFKLTKMFIERGAAGIHMEDQTSTNKKCGHMA
G. intraradices SSTASTSNEPGPDLADYPMDTVPNKVEHLFMAQQFHDRKQRESRFSIS--KEERAKTPFVDYLRPIIADADTGHGGITAILKLTKMFVERGAAGIHVEDQSPSNKKCGHMA
                *:***:::**.*******  * **** **: ** ****** : *            . :*** **:****:****:**::****:*:*:******:***:. .*******


C. cinereus     GKVLVPIQEHINRLVAIRLQYDIMGVENLVVARTDSEAATLITSNIDDRDHPFIQGSTNP-SLPPLNNVMVEAEAQGKTGDQLQAIEDGWIKAANLQLFPQALAQALANEG
E. gossypii     GRCVIPVQEHISRLVTVRMCADVMHSNLVLVARTDSEAATLLSSNIDARDHYYIVGASNPEVTVPLIEVLDAAQQAGASGDRLAQLEEDWCKKAKLRLFHEAFADQVNASP
E. nidulans     GKVLVPISEHINRLVAIRAQADIMGTDLLAIARTDSEAATLITSTIDHRDHPFIIGSTNP-DIQPLNDLMVMAEQAGKNGAELQAIEDEWLAKAGLKLFNDAVVDAINNSP
N. crassa       GKVLVPIQEHINRLVAIRAQADIMGSDLLCIARTDAEAATLITTTIDPRDHAFILGCTNP-DLEPLAHLMMKAEAEGKTGAQLQAIEDDWLAKADLKRFDEAVLDVIAKGK
S. cerevisiae   GRCVIPVQEHVNRLVTIRMCADIMHSDLIVVARTDSEAATLISSTIDTRDHYFIVGATNP-NIEPFAEVLNDAIMSGASGQELADIEQKWCRDAGLKLFHEAVIDEIERS-
G. intraradices GKVLVPISEHINRLIAIRVQFDIMGVNNLIVSRTDSEAATLLTSNIDVRDHAFILGSTNP-NLRPLAEIMQEEEAKGVSGSQLAAIEEKWLSDAKLKLYNDAVIDAIKAS-
                *: ::*:.**:.**:::*   *:*  : : ::***:*****:::.** *** :* *.:**    *: .::     * .* .*  :*: *  * *: : :*. : :


C. cinereus     ASRSTVEKLVARVSRLSW----SQAVAVAQKEFGLKQVPYWNWDAPRTREGYYRYQGGTECAIHRANAFAPYADLLWMETKKPILAQAKEFAAGVHAVHPGQWLAYNLSPS
E. gossypii     SIKDKAGVIAKFNSQIGPQTGASIREMRKLGRELLGQDVYFDWDLPRAREGLYRYKGGTQCAIMRARAFAPYADLVWFESNFPDFQQAKEFAQGVREKFPNKWMAYNLSPS
E. nidulans     LPNKKAAIEKYLTQSKGK----SNLEARAIAKEIAGTDIYFDWEAPRTREGYYRYQGGTQCAINRAVAYAPFADLIWMESKLPDYKQAKEFADGVHAVWPEQKLAYNLSPS
N. crassa       FSNAKDLAAKYQAAVKGKQ--ISNREARAIARQLLGQEIFFDWESPRTREGYYRLKGGCDCSINRAISYAPYCDAIWMESKLPDYAQAEEFAK-GPRVWPEQKLAYNLSPS
S. cerevisiae   ALSNKQELIKKFTSKVGPLTETSHREAKKLAKEILGHEIFFDWELPRVREGLYRYRGGTQCSIMRARAFAPYADLVWMESNYPDFQQAKEFAEGVKEKFPDQWLAYNLSPS
G. intraradices ILPDKNSLLQKWSSQYQG----LSHYNATKLAKSLGVDVFWNWDTPRTREGLYRYQGGTKCAINRAIAYAPYCDLLWMETAKPIRAQAQEFAEGVHKVHPEIMMAYNLSPS
                                                :::*: **.*** ** :** .*:* ** ::**:.* :*:*:  *   **:***       *   ;*******


C. cinereus     FNWKLLPQ-RQDMQAYVWELGKLGFVWQFITLAGLHSNAYISDLFAQNFAKTGMKAYVELVQSRREREIGCDVLTHQKWSGADYADSLIKTVTGGVSSTAAMGAGVTESQFT
E. gossypii     FNWPKAMP-PKEQENYIQRLGEIGYVWQFITLAGLHTNALAIDNFSREFSRFGMRAYAQGIQQREMDEGVDVLKHQKWAGAEYVDSILKLAQGGVSSTASMGKGVTEEQFG
E. nidulans     FNWKKAMP-RDEQETYIKRLGALGYAWQFITLAGLHTTALISDTFAKAYAKQGMRAYGELVQEPEMANGVDVVTHQKWSGANYVDNMLKMITGGVSSTAAMGKGVTEDQFK
N. crassa       FNWKTAMG-RDDQETYIRRLAKLGYCWQFITLAGLHTTALISDQFAKAYSKIGMRAYGELVQEPEIDNGVDVVKHQKWSGATYVDELQKMVTGGVSSTAAMGKGVTEDQFH
S. cerevisiae   FNWPKAMS-VDEQHTFIQRLGDLGYIWQFITLAGLHTNALAVHNFSRDFAKDGMKAYAQNVQQREMDDGVDVLKHQKWSGAEYIDGLLKLAQGGVSATAAMGTGVTEDQFK
G. intraradices FNWDAAGMTDEEIRTYISDLGKLGFVWQFITLGGFHSNALGVDTFARDYKERGMLAYVEGVQRKEREHGVETLQHQKWSGAHYVDRLILTVTGGVNATTAMGKGVTEDQFK
                ***       .: . ::  *. :*: ******.*:*:.*   . *:: : . ** ** : :*  *   * :.: ****:** * * :     ***.:*::** ****.**


C. cinereus     SKL----
E. gossypii     SSNGAKL
E. nidulans     S------
N. crassa       -------
S. cerevisiae   ENGVKK-
G. intraradices K------
```

Figure 2. Multiple alignments of known ICL amino acid sequences from several fungi that were used for designing PCR primers and for comparison with the deduced full-length sequence for ICL from *G. intraradices*. Sequences are shown for: *Coprinus cinereus*, *Eremothecium gossypii*, *Emericella nidulans*, *Neurospora crassa*, *Saccharomyces cerevisiae*, and *G. intraradices*. The degree of homology among the different sequences at each residue is indicated as complete conservation (*), high homology/conserved substitutions (:), moderate conservation (.), or little or no homology (unmarked). Residues shown in bold and underlined are the motifs *RRGT* and *KKFT* that contain Tyr phosphorylation sites in *S. cerevisiae*, shown in bold are the C-terminal tripeptide glyoxysomal-targeting sequences Ser-Lys-Leu (SKL) and AKL in two of the fungal sequences, and another glyoxysomal targeting sequence RDFIAQEQA in the *G. intraradices* sequence. Also underlined in bold is the decapeptide sequence *aveKTKRNYSARD* region that has been shown in *S. cerevisiae* to be involved in Glc-induced enzyme deactivation.

AQ: JJ

Figure 3. Multiple alignments of known MS amino acid sequences from several fungi that were used for designing PCR primers and for comparison with the deduced full-length sequence for ICL from *G. intraradices*. Sequences are shown for *Hansenula polymorpha*, *Candida tropicalis*, *E. nidulans*, *N. crassa*, *S. cerevisiae*, and *G. intraradices*. The degree of homology among the different sequences at each residue is indicated as complete conservation (*), high homology/conserved substitutions (:), moderate conservation (.), or little or no homology (unmarked). Shown in bold are the C-terminal tripeptide glyoxysomal-targeting sequences SKL and AKL that are present in *G. intraradices* and other fungal sequences.

ICL sequence is closely related to ICL sequences from other organisms, having over 60% identity and over 75% similarity to several plant and fungal ICL sequences, including those from the filamentous fungi *E. nidulans* and *N. crassa*. The *G. intraradices* MS sequence is most closely related to the sequence from *E. nidulans*, having 65% identical and 77% similar amino acid residues. The seven sequences with the next highest similarities to the *G. intraradices* MS sequence are also from fungi.

Labeled DNA probes for the *G. intraradices* ICL sequence were used to screen a cDNA library from the extraradical mycelium, and the large number of positive clones found (data not shown) suggest that ICL is also expressed at a substantial level in this tissue. PCR amplification using ICL-specific primers yielded an 800-bp fragment of ICL sequence from unamplified cDNA from mRNA from germinating spores. The same primers yielded a larger fragment, including a small putative intron when genomic DNA from spores was used (not shown).

Quantitative evidence for the expression of the glyoxylate cycle enzymes was obtained by measuring the mRNA levels in extraradical mycelium with fluorescence-based detection of real-time (kinetic) reverse transcriptase (RT)-PCR. As shown in Table I, ICL and MS transcript numbers in this tissue were similar to those of the β-tubulin. Control experiments to evaluate chromosomal DNA contamination in the RNA samples by omission of RT show that less than 1% of the signal can be attributed to DNA across all three samples. T1

Given the large flux of C through the glyoxylate cycle/gluconeogenesis, the significant expression levels of ICL and MS and the putative targeting sequences (see "Discussion") present in MS and ICL of *G. intraradices*, one would expect significant numbers of glyoxysomes in this AM fungus. Therefore, the presence of glyoxysomes was investigated microscopically and electron micrographs of three different zones of *G. intraradices* extraradical hyphae grown under monoxenic conditions are shown in Figure 4. Organelles known to be present in AM external mycelium (Bonfante-Fasolo, 1984; Bago et al., 1998) are easily recognizable, e.g., mitochondria, glycogen deposits, nuclei, and vacuoles. Beside these, some vacuoles with granular matrix and an apparent crystalline, electron-dense core appeared quite frequently (Fig. 4, arrows) in all the hyphal zones observed. These organelles were in the close proximity F4

Table I. *Quantitation of expression of glyoxylate cycle enzymes in extraradical mycelium*

Results of real-time RT-PCR assays performed on duplicate 5-ng samples of RNA isolated from extraradical mycelium. Average threshold cycle (C_T) values represent the no. of PCR cycles required before the signal intensity reaches an arbitrary threshold. C_T values were converted into the absolute copy nos. (mean values ± SD) via standard curves for each assay (not shown). The "No RT" results were obtained from assays using extracted fungal RNA without the reverse transcription step. Likewise, quadruplicate control measurements using no added template for each assay were negative over 45 cycles (not shown).

Gene	No RT Controls		+RT Samples	
	C_T (cycles)	Copies per 5 ng of total RNA	C_T (cycles)	Copies per 5 ng of total RNA
β-Tubulin	35	50 ± 18	26	7,600 ± 430
Isocitrate lyase	33	37 ± 1	26	5,100 ± 270
Malate synthase	33	76 ± 23	25	15,000 ± 6,500

of fungal vacuoles, and they are morphologically identical to microbodies that function as glyoxysomes in other organisms.

Random sequencing of cDNA clones from 11-d germinating *G. intraradices* spores was used to begin the characterization of gene expression profiles in AM fungi. Two hundred ninety-one expressed sequence tags (ESTs) have been deposited in GenBank (dBEST) and these are also available electronically at http://praseo.nmsu.edu/glomus/. A number of these sequences have significant homology to known genes of importance in carbon metabolism. They include an acyl-coenzyme A (CoA) dehydrogenase, Gln-Fru-6-P transaminase, and glycogen-branching enzyme. Other metabolic genes of interest to understanding primary metabolism in the AM symbiosis that were identified by homology to genes of known function include a putative mitochondrial Asp aminotransferase (EC 2.6.1.1) that has 51% identity with the most similar sequence in the database and a spermidine synthase (also known as putrescine aminopropyltransferase, EC 2.5.1.16) that has 60% identity with the gene from *N. crassa*.

DISCUSSION

Gluconeogenic Carbon Flows through the Glyoxylate Cycle

The observation of substantial labeling in C_2 and C_5 of trehalose when $^{13}C_2$ glycerol was provided to the extraradical mycelium or germinating spores indicates an active gluconeogenic flux because C_2 of triose is the precursor of C_2 and C_5 of hexose produced by gluconeogenesis. Gluconeogenesis from labeled triose should label hexose symmetrically with labeling being equal in the two halves of the molecule (carbons 1–3 and 4–6). However, when $^{13}C_2$ glycerol was supplied, the resultant labeling in hexose was asymmetric (compare signals from C_5 and C_2 in Fig. 1, A and B). Although asymmetric labeling in hexose can arise from a lack of equilibration at triose isomerase, this would preferentially label the "top" one-half (C_1–C_3) of hexose, which is made from dihydroxyacetone phosphate (where label from ^{13}C-glycerol enters gluconeogenesis). Because the labeling resulting from exposure to $^{13}C_2$ glycerol is clearly greater in the "lower" one-half ($C_5 > C_2$) of the trehalose rings (Fig. 1, A and B), we may discount disequilibrium at triose isomerase as the cause of asymmetric labeling. The asymmetric labeling and the observed labeling in C_1 and C_3 when $^{13}C_2$ glycerol was provided strongly suggest the action of the PPP on the hexose produced by gluconeogenesis. Substantial activity of a key PPP enzyme (Glc-6-P dehydrogenase) has been directly demonstrated in extracts of another AM fungus (Saito, 1995).

High levels of labeling were also observed in trehalose when $^{13}C_2$-acetate was provided (Fig. 1, C and D), which is consistent with a substantial flux through the glyoxylate cycle. However, incorporation of label into trehalose from acetate is also possible via oxidation of ^{13}C-acetate to $^{13}CO_2$ and refixation during gluconeogenesis. Therefore, it is necessary to compare the labeling in different carbon positions to determine which mechanism is more important.

Labeling from refixation of $^{13}CO_2$ produced by respiration would be predominantly in C_3 and C_4, as was observed previously when germinating spores were exposed to $^{13}CO_2$ (Bago et al., 1999). Trehalose from extraradical mycelium of mycorrhizal cultures exposed to $^{13}CO_2$ also showed labeling predominantly in C_3 and C_4 (spectra not shown), indicating that dark fixation of CO_2 by the fungus is active in the symbiotic state as well. However, when acetate was provided, C_4 was the least labeled position in trehalose. Acetate enters metabolism predominantly at acetyl CoA, and label from $^{13}C_2$-acetate reaching gluconeogenesis through the glyoxylate cycle should end up predominantly in positions 1, 2, 5, and 6 of hexose. Carbons 1, 2, 5, and 6 of trehalose were the most highly labeled in germinating spores and extraradical mycelium. This pattern is consistent with entry of $^{13}C_2$ acetate into acetyl CoA pools followed by flux through citrate synthase to citrate, via aconitase to isocitrate, and then through the glyoxylate cycle steps catalyzed by ICL and MS to malate, followed by scrambling of label through the reversible steps of the TCA cycle between malate and fumarate and finally via gluconeogenesis to hexose.

The fact that when $^{13}C_2$ acetate was provided, the labeling in C_1 and C_2 of trehalose was lower than in C_5 and C_6 and that substantial label appeared in C_3 can be explained by considering the cycling of hexose through PPP as for the glycerol experiments. Once the effects of PPP cycling on label distribution are taken into account, the high degree of labeling in carbohydrate observed when $^{13}C_2$ acetate was supplied can be attributed to a very large flux through the glyoxylate cycle.

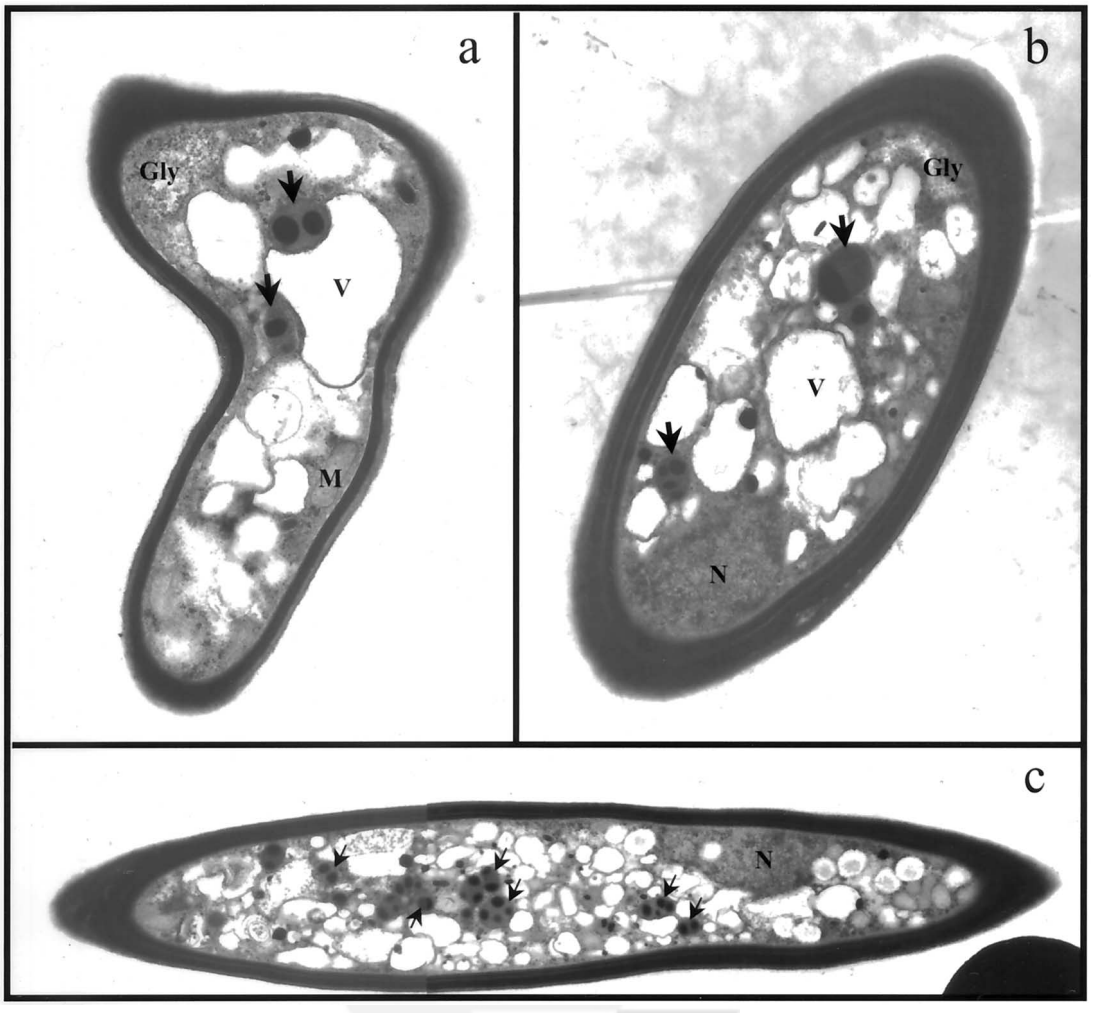

Figure 4. Electron micrographs obtained at different levels of *G. intraradices* extraradical hyphae grown in AM monoxenic cultures. Black solid arrows indicate glyoxysome-like structures, which usually contained electron-dense cores. a, Section near the apex of a branched absorbing structure (BAS). b, Transverse section at the BAS trunk level. c, Longitudinal section of a runner hypha showing a large number of glyoxysome-like organelles. Gly, Glycogen deposits; V, vacuole; M, mitochondrion; N, nucleus. Scale bars are 500 nm in a and b and 1 μm in c.

Implications of the ICL and MS Sequences for Glyoxylate Cycle Regulation and Enzyme Targeting

Because hexose is the form of carbon taken up by AM fungi from plants (Shachar-Hill et al., 1995; Saito et al., 1997; Pfeffer et al., 1999), the possibility of catabolite repression of the glyoxylate cycle by Glc (Jennings, 1995) is an important issue for the regulation of carbon flux in the symbiosis. Labeling experiments showed no evidence for activity of the glyoxylate cycle in the intraradical mycelium where Glc uptake occurs (Pfeffer et al., 1999; Bago et al., 2000). Therefore, we sought evidence for possible regulatory motifs in the ICL sequence from *G. intraradices* by homology with gene sequences from better studied fungi.

ICL is subject to regulation at the level of transcription (Redruello et al., 1999), translation (Dennis et al., 1999; Maeting et al., 1999), enzyme repression (Lopez-Bondo et al., 1987), and proteolytic deactivation (Ordiz et al., 1996). In *S. cerevisiae*, two distinct stages of enzyme inhibition have been characterized (Ordiz et al., 1996). Reversible inhibition occurs within 45 min of exposure to Glc, and this has been linked to phosphorylation of conserved Thr residues by cAMP-dependent protein kinase activity. These Thr residues are part of the motifs RRGT and KKFT in *S. cerevisiae* (see Fig. 2) that are conserved in a number of other fungal species (Maeting et al., 1999). However, the *G. intraradices* ICL we isolated lacks both of these Thr residues. Irreversible inactivation of *S. cerevisiae* ICL by proteolysis in response to external Glc takes roughly four times longer than phosphorylation (Ordiz et al., 1996), and a decapeptide sequence near the amino terminus has been established as being sufficient to confer this Glc-induced degradation (Ordiz et al., 1995). The *G. intraradices* ICL has only modest homology to the yeast sequence in this

decapeptide region (four conserved residues). This degree of homology may be insufficient for Glc-induced inactivation in *G. intraradices* because it appears that ICL in *Ashbya gossypii*, which shares two more homologous residues with the *S. cerevisiae* decapeptide than the *G. intraradices* ICL, is not subject to Glc-induced degradation (Maeting et al., 1999). These comparisons suggest that the mechanisms of Glc-induced regulation of ICL enzymatic activity in yeast may not be the same in AM fungi.

A different mechanism for Glc-induced proteolysis of ICL has recently been described in *E. nidulans* in which the entire peroxisome/glyoxysome is subject to degradation following vacuolar engulfment (Amor et al., 2000). It is interesting that the *G. intraradices* ICL sequence more closely resembles the ICL of *E. nidulans* than of *S. cerevisiae*; for example, within the decapeptide region, seven of 10 residues are the same.

The targeting of proteins to peroxisomes/glyoxysomes has been associated with a C-terminal tripeptide sequence. The sequence SKL was shown to be responsible for the peroxisomal targeting of firefly luciferase (Gould et al., 1989). This tripeptide has been shown to be a member of a group of related sequences—the PTS1-type binding sequences (McNew et al., 1996) that are responsible for specific binding to glyoxisomal membranes (Wolins and Donaldson, 1994). Variations in the PTS1-type tripeptide sequence (Swinkles et al., 1992) include Ala or Cys in place of Ser, His, or Arg for Lys, and Met for Leu. The MS sequence in *G. intraradices* ends with Ala-Arg-Leu. Thus, the Ala-Arg-Leu of MS meets the criteria for being a functional PTS1-type binding sequence, consistent with the idea that this enzyme is targeted to peroxisomes/glyoxysomes in *G. intraradices*.

No PST1-type sequence seems to be present in the ICL C terminus. However, other sequences are associated with peroxisomal/glyoxysomal targeting activity. For example in a yeast amine oxidase, a 16-amino acid N-terminal sequence was shown to be necessary and sufficient for peroxisomal targeting (Faber et al., 1995), whereas the MS of that fungus contains the C-terminal SKL sequence. Also, ICL from castor bean (*Ricinus communis*) that lacks its PST1-type sequence is imported normally into peroxisomes/glyoxysomes (Gao et al., 1996). The sequence of castor bean ICL is the second most similar to that of *G. intraradices*, having 61% identity and 77% similarity. Moreover, tobacco glyoxysomes import proteins with a number of PTS2-type sequences of the form (R or K; 6X; H or Q; A or L or F) near the N terminus (Flynn et al., 1998). The *G. intraradices* ICL has the sequence RDFIAQEQA in positions 4 through 12 (see Fig. 2), so that MS and ICL transcripts contain sequences shown in other organisms to result in peroxisomal/glyoxysomal import.

Expression of Glyoxylate Cycle Genes

The demonstration that ICL and MS are expressed at significant levels is consistent with the NMR observations that indicate a high flux of carbon through the glyoxylate cycle in germinating spores and extraradical mycelium. β-Tubulin was chosen as a reference "housekeeping" gene because it has been found in AM fungi (Astrom et al., 1994) and because its appearance in small scale random sequencing made it likely to be expressed at significant levels in *G. intraradices*. β-Tubulin expression has been followed during development by Butehorn et al. (1999), whose RT-PCR results indicate significant expression levels of this gene in *Glomus mosseae*. RT-PCR has also been used by Requena et al. (2000) to confirm the expression of a putative cell cycle gene in a *G. mosseae*. Thus, our results and those of others show that RT-PCR assays are sufficiently sensitive to measure gene expression in the minute amounts of fungal tissue available from the split-plate culture system (and other culture systems).

Glyoxysomes in AM Fungi

ICL and MS in the majority of fungi, protozoa, and algae are localized in the matrix of cell organelles that are termed "microbodies" (Cioni et al., 1981; Trelease, 1984), or, when functionally defined as containing glyoxylate cycle enzymes, "glyoxysomes." Ultrastructural features of such microbodies are simple and distinctive (Tolbert, 1980; Huang et al., 1983): They are bounded by a single membrane and have a matrix of finely granular or flocculent appearance, and often contain inclusions of variable size, appearing as well-ordered crystalline arrays or as amorphous cores. Microbodies have been observed during the vegetative growth of several filamentous fungi, including *N. crassa* (Desel et al., 1982), *E. nidulans* (Valenciano et al., 1996), and plant phytopathogens *Cladosporium cucumerinum* (Laborda and Maxwell, 1976) and *Fusarium oxysporum* (Werging, 1972). Their presence is related to gluconeogenic metabolism: They proliferate when the fungus is cultured in the presence of acetate or long-chain fatty acids (Veenhuis et al., 1987; Sulter et al., 1990; Valenciano et al., 1996), whereas their numbers sharply decrease when such C stores have been depleted (Tolbert, 1980).

Organelles morphologically identical to those shown in Figure 4 have been seen before in resting spores, young germ tubes, and extraradical hyphae of AM fungi (Sward, 1981a, 1981b; Bonfante et al., 1994; Bago et al., 1998), but in those studies they were described simply as "membrane-bound crystals" or "protein bodies." It is interesting that these organelles were not seen in intraradical AM fungal tissues (Bonfante-Fasolo, 1984), and this is consistent with the fact that the intraradical fungus showed no evidence of gluconeogenic or glyoxylate cycle activity (Pfeffer et al., 1999; Bago et al., 2000).

The putative targeting motifs of MS and ICL and the presence of glyoxysome-like organelles strongly suggest glyoxysomal targeting of ICL and MS in *G. intraradices*. The use of immunohistochemical staining methods would provide additional desirable evidence that MS and/or ICL are so localized.

Metabolic cDNAs Related to Fluxes into and out of the Glyoxylate Cycle

The putative genes for lipid breakdown and glucosamine synthesis, together with a PCR-amplified sequence for glycogen synthase, are currently under investigation together with the carbon fluxes in which they are involved; however, is it noteworthy that their expression in *G. intraradices* is consistent with carbon fluxes into and out of the glyoxylate cycle. Lipid breakdown (lipase and acyl CoA dehydrogenase) provides the acetyl CoA units entering the glyoxylate cycle, whereas synthesis of glycogen and chitin (glycogen synthase, glycogen branching enzyme, and Gln-Fru-6-P transaminase) represent carbohydrate-consuming pathways that use the products of the gluconeogenesis that the glyoxylate cycle feeds.

The detection of a putative Asp amino transferase is consistent with the results of previous labeling studies at this stage of the life cycle in which significant labeling of Glu was observed (Bago et al., 1999). The production of amino acids like Asp and Glu consumes TCA cycle intermediates that need to be replenished. The glyoxylate cycle may serve such an anapleurotic role because the malate produced can replenish TCA cycle intermediates as well as being a gluconeogenic precursor.

The putative spermidine synthase implies synthesis of spermidine from putrescine, whose usual precursor Orn has been detected in *G. intraradices* at
AQ: M significant levels (Johansen et al., 1996). Orn is also made from Arg, which is present at significant levels in this tissue (Bago et al., 1999), and this process may
AQ: N be involved in nitrogen transfer in the AM symbiosis (Bago et al., 2001). The production of Arg also withdraws TCA cycle intermediates and this again may be related to the glyoxylate cycle flux as an anapleurotic pathway.

MATERIALS AND METHODS

Tissue Culture

Extraradical mycelium and spores used for labeling experiments as well as for cDNA library construction were obtained from in vitro cultures of Ri-T DNA transformed roots of carrot (*Daucus carota*) colonized by *Glomus intraradices* (DAOM 197198 Biosystematics Research Center, Ottawa). Conditions for this monoxenic culture were as previously described (St. Arnaud et al., 1996; Pfeffer et al., 1999). In brief, transformed carrot roots were grown together with *G. intraradices* inoculum from a previous monoxenic culture on one side of divided petri plates containing solidified M medium (Chabot et al., 1992). The fungal AQ: O extraradical hyphae, but not the roots, were permitted to grow over the dividing barrier into the other one-half of the plate, which contained M medium without Suc, where they proliferated and sporulated (St. Arnaud et al., 1996). To obtain axenic cultures of *G. intraradices*, spores collected from such plates were germinated in liquid M medium without Suc for 11 to 14 d (1% [w/v] CO_2, 32°C). AQ: P

Isotopic Labeling

Labeling experiments were performed as previously described for the monoxenic (Pfeffer et al., 1999) and for the axenic (Bago et al., 1999) cultures. In brief, to label the extraradical mycelium, ^{13}C-labeled substrates (4 mM $^{13}C_2$ acetate or 10 mM $^{13}C_{1,3}$ glycerol) were added to the fungal compartment approximately 1 week after fungal crossover to the root-free compartment and were grown for 8 weeks at 24°C. The same substrates at the same concentrations were added to germinating spores. Fungal tissue was stored at −80°C after harvest before extraction for NMR analysis or RNA isolation.

NMR Analysis

Extraction of trehalose and other low-M_r water-soluble metabolites was carried out with 70:30 (v/v) methanol: water as previously described (Pfeffer et al., 1999). Extracts were filtered, evaporated under reduced pressure to remove methanol, lyophilized, and redissolved in deuterated water for NMR spectroscopy. Conditions and instrumentation for obtaining NMR spectra were as previously described (Bago et al., 1999; Pfeffer et al., 1999) using 400-MHz instruments (Varian, Palo Alto, CA) for ^{13}C and a 750-MHz instrument (Bruker Instruments, Billerica, MA) for ^{1}H spectroscopy. The total percentage of ^{13}C at each carbon position of trehalose was determined by using the ^{1}H spectra to assign absolute ^{13}C content in C_1 and ^{13}C spectra to determine relative ^{13}C content in the other positions. Restrictions on the availability of 750 MHz instrument time meant that 1H spectra were not run on all samples, and the percentage of ^{13}C levels quoted in the "Results" and "Discussion" are for one representative set of samples for which ^{1}H spectra were run. For the others (n = 3 for each experimental conditions), ^{13}C spectra showed that the relative ^{13}C enrichments in the different carbon positions of trehalose were the same to within ±10% as those for the samples whose absolute ^{13}C contents are quoted in the text.

RNA Extraction

Total RNA was isolated using a modified hot phenol/SDS method (Wilkins and Smart, 1996) followed by CsCl AQ: Q ultracentrifugation (Maniatis et al., 1989). The germinated AQ: R spores were harvested and ground to a fine powder with sand under liquid nitrogen. The ground tissue was resuspended in a 1:2 mixture of hot (65°C) phenol and lysis

buffer (0.1 M Tris, 0.1 M LiCl, 5 mM EDTA, 0.1 M NaCl, 0.1 M sodium acetate, 1% [w/v] SDS, and β-mercaptoethanol, pH 5.2). The suspension was incubated for 10 min at 65°C with occasional vortexing. One-fourth volume of chloroform:isoamyl alcohol (24:1, v/v) was added, and the aqueous phase was recovered following centrifugation. The aqueous phase was extracted repeatedly with hot phenol (pH 4.5) and phenol:chloroform:isoamyl alcohol (25:24:1, v/v) until there was no interphase. To the cleaned aqueous phase, guanidine thyocyanate was added to make 4 M solution and was ultracentrifuged in the presence of CsCl. The RNA pellet was washed with 70% (w/v) ethanol, dissolved in Tris-EDTA, and stored at −80°C.

EST Library Construction

A cDNA library from 11-d-old germinating *G. intraradices* spores was constructed using the SMART kit (CLONTECH, Palo Alto, CA). One microgram of total RNA served for first strand cDNA synthesis, and the resulting single-stranded cDNA was amplified by PCR. After digestion with *Sfi*I and size fractionation, the cDNA was ligated into the *Sfi*I-digested λTriplEx2 vector, which contains the asymmetrical *Sfi*I sites (A&B) in the multicloning site. The ligated cDNA was packaged using Gigapack III λ extract (Stratagene, La Jolla, CA). The library was titered on *Escherichia coli* strain XL1-Blue using NZCYM plates with 0.7% (w/v) top agar containing 2.5 mM isopropyl-β-D-thiogalactopyranoside and 2.5 mM 5-bromo-4-chloro-3-indolyl-β-D-galactopyranoside.

cDNA Sequencing and Analyses

λTriplEx2 clones were converted to pTriplEx2 plasmid using *E. coli* BM25.8 as the bacterial host. Plasmid DNA was prepared using QIAprep spin miniprep kit (Qiagen, Valencia, CA). The lengths of individual cDNA inserts were determined by digestion of the prepared plasmid DNA with the restriction enzyme *Sfi*I. Nucleotide sequences of the cDNA inserts were determined with the dideoxy chain-termination method using SequiTherm Excel II kit (Epicentre Technologies, Madison, WI). Tpx and T7 primers were used to generate 5′ and 3′ sequence information, respectively. The sequence information was obtained from 4200 IR^2 automated sequencers (LI-COR) using 66-cm plates with 4% (w/v) acrylamide and 7 M urea gels.

The longest usable sequence read was 1,062 bp, whereas the shortest was 148 bp. The DNA sequences from each clone were compiled into a single FASTA format to create a unique *G. intraradices* EST database on a UNIX workstation for local BLAST similarity searching. Each sequence in this database was compared with every other sequence in the database and was sorted to determine the number of unique and repetitive clones. rRNA sequences were removed. Sixty-one sequence files had at least one significant BLASTN match in the *G. intraradices* database, the largest group of which contained nine overlapping sequences. Sequences were end trimmed to remove low-quality base calls. Of the 291 EST sequences deposited, 267 (91.7%) were composed of greater than 92% unambiguous base calls, with mean and median being 96%. Only one sequence contained less than 80% unambiguous base calls (77%).

All sequences in the *G. intraradices* database were compared against the GenBank NonRedundant database (National Center for Biotechnology Information [NCBI], Bethesda, MD) using BLASTX. The definition lines from the best matches to each sequence having an E value less than 1e-5 were parsed to the COMMENT field in the dbEST header for each sequence. If the best E value was less that 1e-20, and all the top hits corresponded to genes of the same function, then a descriptor was pasted into the PUTITIVE-ID: field of the dbEST entry. Vector sequences were removed prior to deposition with NCBI dbEST. The sequences are available from NCBI with dbEST accession numbers from 5812585 to 5812875 and GenBank numbers from BE603746 to BE604036. They are also available at http://praseo.nmsu.edu/glomus/.

PCR for Gene Isolation

To amplify the genes of ICL and MS from *G. intraradices*, a series of fungal amino acid sequences for each gene was aligned using CLUSTAL W program. Degenerate PCR primers of 20 nucleotides were designed based on regions of high sequence conservation as follows: 5′ ICL, 5′AARTGYGGNCAYATGGCNGG3′; 3′ ICL, 5′-GCNARNGTDATRAAYTGCCA-3′; 5′ MS, 5′-CARRTNAAYYTNTAYGAYGC-3′; and 3′ MS, 5′-GARGAYGCNGCNACNGCNGA-3′.

cDNA from 11-d germinating spores of *G. intraradices* served as template. The PCR product was cloned into Topo vector (Invitrogen, Carlsbad, CA), and the plasmid DNA of random clones were isolated and sequenced.

Screening of EST Libraries

The *G. intraradices* libraries of germinating spores and extraradical hyphae (gift from Dr. Maria Harrison, Noble Foundation, Ardmore, OK) were screened with digoxigenin-dUTP-labeled (Roche, Basel) cDNA probes. About 200,000 plaques were screened from each library and the plaque lifts were made according to Maniatis et al. (1989).

Obtaining Full-Length Sequences by RACE

Full-length cDNA sequences were obtained using the SMART RACE cDNA amplification kit (CLONTECH). Two hundred-fifty nanograms of total RNA was used to synthesize each 5′- and 3′-RACE-ready cDNA. The sequences of gene-specific primers employed for RACE were based on the sequences of gene fragments obtained from PCR-based amplification of fragments (described above) and were synthesized by IDT, Inc (XXXX, XX). Primer sequences were as follows: 5′ ICL, 5′-GCGTCACTCAACCACTTCTCTTCTATCGCAGC-3′; 3′ ICL, 5′-GCGGTCATATGGCTGGAAAAGTATTGGTGCCG-3′; 5′ MS, 5′- TGGATTGGTACACAAC-

CAAGTCCACGTAACC-3′; and 3′ MS, 5′- GCTGGAC-ATGATGGTACTTGGGTTGCACATCC-3′.

The resulting RACE fragments for each gene were cloned into the pGEM-T Easy vector (Promega, Madison, WI) and were sequenced with M13 forward and reverse primers.

Real-Time RT-PCR Quantification of Gene Expression

The extraradical mycelium from the fungal compartments of two sets of three plates were weighed (15 and 20 mg), and from these, RNA extraction yielded 240 and 270 ng of total RNA, respectively. Gene expression was monitored using an PRISM 7700 instrument (Applied Biosystems, Foster City, CA) and "Taqman" assays designed for β-tubulin, ICL, and MS. The amplification and probe sequences for each assay are shown below along with amplicon sizes and the region of each cDNA amplified in parentheses. Primers were used at 500 nM and probes at 100 nM final concentrations. Absolute quantification was based on standard curves for each assay. Plasmid DNA containing each amplicon was prepared using Qiagen kits and was quantified by UV absorbance spectroscopy. Standard curves were determined from duplicate samples at 10^2, 10^3, 10^4, and 10^6 copies for each assay (not shown).

β-Tubulin (316-397) 88 bp

AQ: AA Forward primer, 5′-AGAAAGTCTACCACGGAAAAT-AGTAGCT-3′; reverse primer, 5′-TTCACGTAATATGAT-GGCTGCAT-3′; and Taq-Man probe, 5′-FAM-CGGTC-AAATATCTTCCATGACGAGGATCG-TAMRA-3′.

ICL (787-869) 83 bp

AQ: BB Forward primer, 5′-TGCTACTCTTCTCACATCTAA-CATCGA-3′; reverse Primer, 5′-CAAGAGGGCGAAGGT-TAGGA-3′; and Taq-Man Probe, 5′-FAM-TCCGAGATCA-CGCGTTCATTCTTGG3′-TAMRA-3′.

MS (1,354-1,430) 77 bp

AQ: CC Forward primer, 5′-TTGGTTGTGTACCAATCCATA-ATCTT-3′; reverse primer, 5′-CCATTGCCATAATTGT-GAACGT-3′; and Taq-Man Probe: 5′-FAM-TTTCTGCTGT-TGCCGCATCTTCCA-TAMRA-3′.

To prepare template for RT-PCR assays, 100 ng of total RNA was treated with RNase-free DNase-I (DNA free; Ambion, Austin, TX) for 1 h followed by DNase-I removal as specified by the manufacturer. Duplicate assays used 5-ng aliquots of the DNase-treated RNA preincubated for 15 min at 95°C then placed on ice to remove any potential interfering secondary structures. The reverse amplification primer served as the primer for reverse transcription. Each RT-PCR assay was run in 50 mL of total volume using One-Step RT-PCR Master mix containing AmpliTaq Gold DNA polymerase to which 12.5 units of MultiScribe enzyme was added (all from Applied Biosystems). The reactions were incubated at 48°C for 60 min for reverse transcription, followed by a 10-min incubation at 95°C to activate the AmpliTaq Gold polymerase and 45 cycles of 15 s at 95°C, and 1 min at 60°C. MultiScribe enzyme was omitted from the no-RT control reactions.

Ultrastructural Observations

Four-week-old extraradical hyphae growing within the monoxenic culture medium were prepared for electron microscopy imaging according to Bago et al. (1998). In brief, small agar cubes containing non-septated external hyphae were incubated overnight at 4°C in a solution containing 2% (w/v) glutaraldehyde and 2% (w/v) formaldehyde in 0.1 M cacodylate buffer (pH 7.2). After fixation, agar cubes were rinsed in a cacodylate buffer solution for 3 to 12 h. The buffer was changed three times. Samples were then postfixed with 1% (w/v) osmium tetroxide in the same buffer for 2 h, dehydrated in ethanol, and embedded in Epon 812. Serial sections of the specimens were taken at different levels of extraradical hyphae, but preferentially at the so-called BAS (Bago et al., 1998). Observations were carried out with a 1,200× electron microscope (JEOL, Tokyo).

Concluding Remarks

Huge fluxes of photosynthate move from plants to AM fungi globally. Much of this carbon is converted to lipids by the fungus within mycorrhizal roots and is exported to the extraradical mycelium. The results of this study provide strong evidence for a large metabolic flux through the glyoxylate cycle, as well as for the expression of genes for ICL and MS, the two key enzymes of this metabolic pathway, in an AM fungus. Putative glyoxysomes were identified in regions in which we expect lipid utilization, in agreement with putative glyoxysomal targeting motifs in the enzyme sequences. We conclude that the glyoxylate cycle has a central role in the utilization by the fungus of carbon exported from the host plant in this AM symbiosis.

ACKNOWLEDGMENTS

The authors thank the technical support provided by Alain Goulet (Université Laval, Quebec, Canada) on electron microscopy imaging, and Janine Brouillette on NMR AQ: DD spectroscopy. We thank Dr. Paola Bonfante for expert comments on micrograph interpretation.

Received April 19, 2001; returned for revision May 16, 2001; accepted June 18, 2001.

LITERATURE CITED

Amor C, Dominguez AI, De Lucas JR, Laborda F (2000) The catabolite inactivation of *Aspergillus nidulans* isocitrate lyase occurs by specific autophagy of peroxisomes. Arch Microbiol **174:** 59–66

Astrom H, Giovannetti M, Raudaskoski M (1994) Cytoskeletal components in the arbuscular mycorrhizal

fungus *Glomus mosseae*. Mol Plant-Microbe Interact **7:** 309–312

Bago B, Azcón-Aguilar C, Goulet A, Piché Y (1998) Branched absorbing structures (BAS): a feature of the extraradical mycelium of symbiotic arbuscular mycorrhizal fungi. New Phytol **139:** 375–388

Bago B, Pfeffer PE, Douds DD, Brouillette J, Bécard G, Shachar-Hill Y (1999) Carbon metabolism in spores of the arbuscular mycorrhizal fungus *Glomus intraradices* as revealed by nuclear magnetic resonance spectroscopy. Plant Physiol **121:** 263–271

Bago B, Pfeffer PE, Shachar-Hill Y (2000) Carbon metabolism and transport in arbuscular mycorrhizas. Plant Physiol (in press)

AQ: EE

Bago B, Pfeffer PE, Shachar-Hill Y (2001) Could the urea cycle be translocating nitrogen in the arbuscular mycorrhizal symbiosis? New Phytol (in press)

AQ: FF

Bécard G, Doner LW, Rolin DB, Douds DD, Pfeffer PE (1991) Identification and quantification of trehalose in vesicular-arbuscular mycorrhizal fungi by in vivo 13C NMR and HPLC analyses. New Phytol **118:** 547–552

Beilby JP, Kidby DK (1980) Biochemistry of ungerminated and germinated spores of the vesicular-arbuscular mycorrhizal fungus, *Glomus caledonium*: changes in neutral and polar lipids. J Lipid Res **21:** 739–750

Bonfante P, Balestrini R, Mendgen K (1994) Storage and secretion processes in the spore of *Gigaspora margarita* Becker and Hall as revealed by high-pressure freezing and freeze substitution. New Phytol **128:** 93–101

Bonfante-Fasolo P (1984) Anatomy and morphology of VA mycorrhizae. *In* CL Powell, DJ Bagyaraj, eds, VA Mycorrhiza. CRC Press, Boca Raton, FL, pp 5–33

Butehorn B, Gianinazzi-Pearson V, Franken P (1999) Quantification of β-tubulin RNA expression during asymbiotic and symbiotic development of the arbuscular mycorrhizal fungus *Glomus mosseae*. Mycol Res **103:** 360–364

Chabot S, Bécard G, Piche Y (1992) Life-cycle of *Glomus intraradix* in root organ-culture. Mycologia **84:** 315–321

Cioni M, Pinzauti G, Vanni P (1981) Comparative biochemistry of the glyoxylate cycle. Comp Biochem Physiol B **70B:** 1–26

Desel H, Zimmermann M, Miller JF, Neupert W (1982) Biosynthesis of glyoxysomal enzymes in *Neurospora crassa*. Ann N Y Acad Sci **386:** 377–389

Ezawa T, Saito M, Yoshida T (1995) Comparison of phosphatase localization in the intraradical hyphae of arbuscular mycorrhizal fungi *Glomus* spp. and *Gigaspora* spp. Plant Soil **176:** 56–63

Faber KN, Keizergunnink I, Pluim D, Harder W, Ab G, Veenhuis M (1995) The N terminus of amine oxidase of *Hansenula polymorpha* contains a peroxisomal targeting signal. FEBS Lett **357:** 115–120

Flynn CR, Mullen RT, Trelease RN (1998) Mutational analyses of a type 2 peroxisomal targeting signal that is capable of directing oligomeric protein import into tobacco BY-2 glyoxysomes. Plant J **16:** 709–720

Franken P, Lapopin L, MeyerGauen G, GianinazziPearson V (1997) RNA accumulation and genes expressed in spores of the arbuscular mycorrhizal fungus, *Gigaspora rosea*. Mycologia **89:** 293–297

Gao XP, Marrison JL, Pool MR, Leech RM, Baker A (1996) Castor bean isocitrate lyase lacking the putative peroxisomal targeting signal 1 ARM is imported into plant peroxisomes both in vitro and in vivo. Plant Physiol **112:** 1457–1464

Gaspar L, Pollero R, Cabello M (1997) Partial purification and characterization of a lipolytic enzyme from spores of the arbuscular mycorrhizal fungus *Glomus versiforme.* Mycologia **89:** 610–614

Graham JH (2000) Assessing costs of arbuscular mycorrhizal symbiosis agroecosystems fungi. *In* GK Podila, DD Douds Jr, eds, Current Advances in Mycorrhizae Research. APS Press, St. Paul, pp 127–140

Harrier LA, Wright F, Hooker JE (1998) Isolation of the 3-phosphoglycerate kinase gene of the arbuscular mycorrhizal fungus *Glomus mosseae* (Nicol. & Gerd.) Gerdemann & Trappe. Curr Genet **34:** 386–392

Harrison MJ (1999) Molecular and cellular aspects of the arbuscular mycorrhizal symbiosis. Annu Rev Plant Physiol **50:** 361–389

Huang AHC, Trelease RN, Moore TS (1983) Plant Peroxysomes. Academic Press, New York

Jabaji-Hare S (1988) Lipid and fatty acid profiles of some vesicular-arbuscular mycorrhizal fungi: contribution to taxonomy. Mycologia **80:** 622–629

Jennings DH (1995) The Physiology of Fungal Nutrition. Cambridge University Press, London

Johansen A, Finlay RD, Olsson PA (1996) Nitrogen metabolism of the external hyphae of the arbuscular mycorrhizal fungus *Glomus intraradices*. New Phytol **133:** 705–712

Kaldorf M, Schmelzer E, Bothe H (1998). Expression of maize and fungal nitrate reductase genes in arbuscular mycorrhiza. Mol Plant-Microbe Interact **11:** 439–448

Kojima T, Hayatsu M, Saito M (1998) Intraradical hyphal phosphatase of the arbuscular mycorrhizal fungus *Gigaspora margarita*. Biol Fertil Soil **26:** 331–335

Laborda F, Maxwell DP (1976) Ultrastructural changes in *Cladosporium cucumerinum* during pathogenesis. Can J Microbiol **22:** 394–403

Lanfranco L, Garnero L, Bonfante (1999) Chitin synthase genes in the arbuscular mycorrhizal fungus *Glomus versiforme*: full sequence of a gene encoding a class IV chitin synthase. FEMS Microbiol Lett **170:** 59–67

MacDonald RM, Lewis M (1978) The occurrence of some acid phosphatases and dehydrogenases in the vesicular-arbuscular mycorrhizal fungus *Glomus mosseae*. New Phytol **80:** 135–141

Maeting I, Schmidt G, Sahm H, Revuelta JL, Stierhof YD, Stahmann KP (1999) Isocitrate lyase of *Ashbya gossypii*: transcriptional regulation and peroxisomal localization. FEBS Lett **444:** 15–21

Nemec S (1981) Histochemical characteristics of *Glomus etunicatus* infection of *Citrus limon* fibrous roots. Can J Bot **59:** 609–617

Ordiz I, Herrero P, Rodicio R, Moreno F (1995) Glucose-induced inactivation of isocitrate lyase in *Saccharomyces*

cerevisiae is mediated by an internal decapeptide sequence. FEBS Lett **367:** 219–222

Ordiz I, Herrero P, Rodicio R, Moreno F (1996) Glucose-induced inactivation of isocitrate lyase in *Saccharomyces cerevisiae* is mediated by the camp-dependent protein kinase catalytic subunits tpk1 and tpk2. FEBS Lett **385:** 43–46

Pfeffer PE, Douds DD, Bécard G, Shachar-Hill Y (1999) Carbon uptake and the metabolism and transport of lipids in and arbuscular mycorrhiza. Plant Physiol **120:** 587–598

Redecker D, Kodner R, Graham LE (2000a) Glomalean fungi from the Ordovician. Science **289:** 1920–1921 AQ: GG

Redecker D, Morton JB, Bruns TD (2000b) Ancestral lineages of arbuscular mycorrhizal fungi (Glomales). Mol Phylog Evol **14:** 276–284

Requena N, Mann P, Franken P (2000) A homologue of the cell cycle check point TOR2 from *Saccharomyces cerevisiae* exists in the arbuscular mycorrrhizal fungus *Glomus mosseae*. Protoplasma **212:** 89–98

Saito M (1995) Enzyme activities of the internal hyphae and germinated spores of an arbuscular mycorrhizal fungus, *Gigaspora margarita* Becker & Hall. New Phytol **129:** 425–431

Schubert A, Wyss P (1995) Trehalase activity in mycorrhizal and non-mycorrhizal roots of leak and soybean. Mycorrhiza **5:** 401–404

Shachar-Hill Y, Pfeffer PE, Douds D, Osman SF, Doner LW, Ratcliffe RG (1995) Partitioning of intermediate carbon metabolism in VAM colonized leek. Plant Physiol **108:** 7–15

Simon L (1996) Phylogeny of the Glomales: deciphering the past to understand the present. New Phytol **133:** 95–101 AQ: HH

Simon L, Bousquet J, Lévesque RC, Lalonde M (1993) Origin and diversification of endomycorrhizal fungi and coincidence with vascular land plants. Nature **363:** 67–69

Smith SE, Read DJ (1997) Mycorrhizal Symbiosis. Academic Press, London

St. Arnaud M, Hamel C, Vimard B, Caron M, Fortin JA (1996) Enhanced hyphal growth and spore production of the arbuscular mycorrhizal fungus *Glomus intraradices* in an *in vitro* system in the absence of host roots. Mycol Res **100:** 328–332

Sulter GJ, Waterham HR, Goodman JM, Veenhuis M (1990) Proliferation and metabolic significance of peroxysomes in *Candida boidinii* during growth on D-alanine or oleic acid as the sole carbon source. Arch Microbiol **153:** 485–489

Sward RJ (1981a) The structure of the spores of *Gigaspora margarita*: I. The dormant spore. New Phytol **87:** 761–768

Sward RJ (1981b) The structure of the spores of *Gigaspora margarita*: III. Germ-tube emergence and growth. New Phytol **88:** 667–673

Taylor TN, Remy W, Hass H, Kerp H (1995) Fossil arbuscular mycorrhizae from the early Devonian. Mycologia **87:** 560–573

Tolbert NE (1980) Microbodies-peroxysomes and glyoxysomes. *In* PK Strumpf, EE Conn, eds, The Biochemistry of Plants. Academic Press, New York, pp 359–388

Valenciano S, De Lucas JR, Pedregosa A, Monistrol IF, Laborda F (1996) Induction of b-oxidation enzymes and microbody proliferation in *Aspergillus nidulans*. Arch Microbiol **166:** 336–341

Veenhuis M, Douma A, Harder W, Osumi M (1983) Degradation and turnover of peroxysomes in the yeast *Hansenula polymorpha* induced by selective inactivation of peroxysomal enzymes. Arch Microbiol **134:** 193–203 AQ: II

Veenhuis M, Matelblowski M, Kunau WH, Harder W (1987) Proliferation of microbodies in *Saccharomyces cerevisiae*. Yeast **3:** 77–84

Werging WP (1972) Ultrastructural comparison of microbodies in pathogenic and saprophytic hyphae of *Fusarium oxysporum* f. sp. *lycopersici*. Phytopathology **62:** 1045–1051

Wolins NE, Donaldson RP (1994) Specific binding of the peroxisomal protein targeting sequence to glyoxysomal membranes. J Biol Chem **269:** 1149–1153